



## Crystal transition from cellulose II hydrate to cellulose II

Kayoko Kobayashi<sup>a</sup>, Satoshi Kimura<sup>a,b</sup>, Eiji Togawa<sup>c</sup>, Masahisa Wada<sup>a,b,\*</sup>

<sup>a</sup> Department of Biomaterials Science, Graduate School of Agricultural and Life Sciences, The University of Tokyo, Tokyo 113-8657, Japan

<sup>b</sup> Department of Plant & Environmental New Resources, College of Life Sciences, Kyung Hee University, 1, Seocheon-dong, Giheung-ku, Yongin-si, Gyeonggi-do 446-701, Republic of Korea

<sup>c</sup> Forestry and Forest Products Research Institute, Matsunosato 1, Tsukuba, Ibaraki 305-8687, Japan

### ARTICLE INFO

#### Article history:

Received 6 April 2011

Received in revised form 24 May 2011

Accepted 25 May 2011

Available online 1 June 2011

#### Keywords:

Cellulose II hydrate

Cellulose II

Synchrotron X-ray fiber diffraction

Solid-state <sup>13</sup>C NMR

Crystal transition

### ABSTRACT

Samples of cellulose II hydrate were prepared by immersion of mercerized cellulose II in anhydrous hydrazine followed by washing with water. The synchrotron X-ray fiber diffraction and solid-state <sup>13</sup>C NMR measurements showed that cellulose II hydrate had a larger unit cell that contained water molecules with lower degree of crystallinity than mercerized cellulose II, but it had basically the same molecular conformation as mercerized cellulose II. The crystal transition from cellulose II hydrate to cellulose II was monitored using synchrotron X-ray diffraction under controlled relative humidity. In the drying process, the cellulose II hydrate gradually contracted, and this decreased the distance between the hydrophobic stacking sheets of molecular chains, while maintaining its sheet structure. The absence of an obvious transition point and the irreversibility of the transition indicated a random location of the water molecules occurred in the unit cell of cellulose II hydrate. On annealing a sample in hot water, the cellulose II hydrate was converted to cellulose II. Cellulose II hydrate was unstable at high temperatures, even in water.

© 2011 Elsevier Ltd. All rights reserved.

### 1. Introduction

Hydrate forms of cellulose have been studied since they were first identified by Sakurada and Hutino (1936). Two structures that can be prepared in different ways are known to exist: Na–cellulose IV and cellulose II hydrate. Na–cellulose IV is one of the intermediates of the mercerization process (Okano & Sarko, 1984, 1985; Porro, Bédoué, Chanzy, & Heux, 2007). Mercerization is an alkali treatment of native cellulose, which causes a transition to occur from the native cellulose (cellulose I<sub>α</sub> and I<sub>β</sub>) (Atalla & VanderHart, 1984; VanderHart & Atalla, 1984) to cellulose II. In this process, cellulose initially swells on immersion in an alkali solution to form a complex with alkali ions and water molecules that is known as Na–cellulose I. As a result of washing this complex with water, the alkali is washed out of the crystalline lattice, causing it to convert into Na–cellulose IV. Nishimura and Sarko (1991) determined the crystal structure of Na–cellulose IV using X-ray diffraction and stereochemical modeling. The proposed model of Na–cellulose IV has an antiparallel chain packing, with a two-chain monoclinic P2<sub>1</sub> unit cell ( $a = 8.72 \text{ Å}$ ,  $b = 9.57 \text{ Å}$ ,  $c = 10.35 \text{ Å}$ , and  $\gamma = 122.0^\circ$ ), where two water molecules are regularly located between the corner chains, forming hydrogen bonds with adjacent cellulose chains.

On the other hand, the other hydrate form of cellulose, cellulose II hydrate, is obtained by washing a cellulose II–hydrazine complex with water. Lee and Blackwell (1981a) described the structure of cellulose–hydrazine complexes formed by immersion of cellulose in anhydrous hydrazine, and they found that the hydrate form could be prepared from a decomposition process from the cellulose II–hydrazine complex to cellulose II by washing it with water. Subsequently, Lee and Blackwell further studied the crystal structure of cellulose II hydrate using X-ray diffraction and stereochemical modeling based on the cellulose II structure (Lee & Blackwell, 1981b). The refined model was described based on a two-chain monoclinic P2<sub>1</sub> unit cell ( $a = 9.02 \text{ Å}$ ,  $b = 9.63 \text{ Å}$ ,  $c = 10.34 \text{ Å}$ , and  $\gamma = 116.0^\circ$ ) with an antiparallel arrangement. In the unit cell, four water molecules were randomly present between the hydrophobic stacking sheets of the molecular chains.

These two hydrate forms of cellulose have a common property in that they are converted to cellulose II on dehydration. In comparison with the monoclinic unit cell of mercerized cellulose II ( $a = 8.10 \text{ Å}$ ,  $b = 9.03 \text{ Å}$ ,  $c = 10.31 \text{ Å}$ , and  $\gamma = 117.10^\circ$ ) (Langan, Nishiyama, & Chanzy, 2001), their unit cells are expanded to include the water molecules, but both structures have a similar basic molecular conformation and stacking as cellulose II. However, structural studies have shown that Na–cellulose IV and cellulose II hydrate differ in some ways, such as in the size of their unit cells and the arrangement of water molecules.

Recently, we have reexamined the crystal structure of Na–cellulose IV prepared from ramie fibers using synchrotron X-ray diffraction and solid-state <sup>13</sup>C NMR spectroscopy. We have also

\* Corresponding author at: Department of Biomaterials Science, Graduate School of Agricultural and Life Sciences, The University of Tokyo, Tokyo 113-8657, Japan. Tel.: +81 3 5841 5247; fax: +81 3 5841 2677.

E-mail address: [awadam@mail.ecc.u-tokyo.ac.jp](mailto:awadam@mail.ecc.u-tokyo.ac.jp) (M. Wada).

monitored the crystal transition from Na–cellulose IV to cellulose II using X-ray diffraction (Kobayashi, Kimura, Togawa, & Wada, 2011). This study provided an understanding of the nature of the transition and the mechanism of the transition, and provided an indication of the random location of any water molecules, but was inconsistent with the previous X-ray study of Nishimura and Sarko (1991). Therefore, in this study, we carried out a similar analysis on cellulose II hydrate to examine the crystal structure, the nature of the transition, and the mechanism of the transition, comparing them with the case of Na–cellulose IV. In addition, the stability at high temperatures was investigated to obtain a further understanding of this compound's stability.

## 2. Experimental

### 2.1. Sample preparation

A bundle of purified ramie fibers, supplied by the Teikoku Boseki Co. (Japan), was aligned and fixed to a stainless steel stretching device. The fibers were immersed in a 5 N NaOH solution and washed with deionized water. Subsequently, the fibers were immersed in a 3 N NaOH solution and repeatedly washed with ice water, as reported in previous studies (Langan et al., 2001; Hori & Wada, 2006). The mercerized cellulose II fibers were then immersed in anhydrous hydrazine for 2 d at 4 °C. Samples of cellulose II hydrate were prepared by thoroughly washing hydrazine treated fibers in deionized water. The samples were kept in water to maintain the hydrate form or kept over P<sub>2</sub>O<sub>5</sub> in a desiccator to dehydrate the samples. The fibers were stretched along the fiber axis in all the above treatments.

### 2.2. Synchrotron X-ray fiber diffraction analysis

Synchrotron X-ray fiber diffraction was carried out at the BL38B1 beam line located at the SPring-8 facility (Hyogo, Japan). The oriented fibers were mounted on a goniometer head and synchrotron-radiated X-rays ( $\lambda = 1 \text{ \AA}$ ) were irradiated for a period of 120 s orientated orthogonal to the fiber axis. In the measurements on cellulose II hydrate, air with a RH = 90% generated using a humidity generator (Shinyei SRG-1R, Japan), was allowed to flow over the sample to maintain it in the wet condition. The fiber patterns were recorded using a camera system equipped with a flat imaging plate (IP) (R-Axis V, Rigaku) at room temperature. The sample-to-IP distance was calibrated using Si powder ( $d = 0.31355 \text{ nm}$ ). The peak positions of the fiber diffraction patterns were measured using the R-Axis display software package (Rigaku). After indexing the  $d$ -spacings, the unit-cell parameters were determined using a least-squares method.

### 2.3. Solid-state CP/MAS <sup>13</sup>C NMR spectroscopy

Solid-state <sup>13</sup>C NMR spectra were obtained using a CMX 300 spectrometer (Chemagnetics, USA) operating at 75.6 MHz. The sample was placed in a 4.0 mm zirconia rotor, and was spun at a frequency of 5 kHz in a solid-state probe at the magic angle. All the spectra were obtained using a <sup>1</sup>H NMR 90° pulse length of 2.5  $\mu$ s, with a cross-polarization time of 1.0 ms and a 60 kHz CW proton decoupling. The recycle time was 3 s. The spectra were calibrated using adamantane as a standard. The rotor was sealed using a Teflon cap to avoid any drying out of the cellulose II hydrate sample.

### 2.4. Monitoring of the crystal transition using synchrotron X-ray diffraction

Monitoring of the drying of cellulose II hydrate was carried out in the BL40B2 beam line at the SPring-8 facility (Hyogo, Japan).

The oriented sample of cellulose II hydrate was mounted on a goniometer head in flowing humidity-controlled air generated by a humidity generator (Shinyei SRG-1R) at a flow rate of 1 L min<sup>-1</sup>, and synchrotron-radiated X-rays ( $\lambda = 0.7 \text{ \AA}$ ) were irradiated for a period of 120 s orientated orthogonal to the fiber axis. The fiber patterns were recorded on a flat imaging plate (R-Axis V<sup>++</sup>, Rigaku). The measurements were performed from RH = 100–0% in decreasing steps of 10%. The sample that had dried at RH = 0% was subsequently wetted using a few drops of water, and the measurements were performed again at RH = 100%. Each X-ray diffraction measurement was carried out after a stabilization time of 10 min.

The equatorial and meridional X-ray diffraction profiles at each RH step were obtained by analyzing the fiber diffraction diagrams using the R-Axis display software package (Rigaku). The peak positions were determined by peak fitting the X-ray diffraction profiles, as reported previously (Wada, Okano, & Sugiyama, 1997).

### 2.5. Examination of the reversibility of the crystal transition using X-ray diffractometry

X-ray diffractometry in the reflection mode was carried out using a Rigaku RINT2000 diffractometer (Rigaku, Japan), employing monochromatic Cu K $\alpha$  radiation ( $\lambda = 1.5418 \text{ \AA}$ ), generated at 38 kV with an excitation current of 50 mA, using an optical slit system: divergence slit = 0.5°; scattering slit = 0.5°; and receiving slit = 0.15 mm. Humidity-controlled nitrogen gas generated by a humidity generator (Shinyei SRG-1R) was introduced into the goniometer sealed with a polyester (Mylar) film at a flow rate of 1 L min<sup>-1</sup>. The fibers of cellulose II hydrate were placed in the goniometer at RH = 100%, and the scanning was performed using a scattering angle of  $2\theta = 5\text{--}30^\circ$  with a step size of  $2\theta = 0.1^\circ$  and an accumulation time of 10 s. After the measurements were obtained, the sample was dried under a RH = 50% for a period of a few hours, and then the scanning was carried out once again. Finally, the sample was rehydrated under a RH = 100% for a period of a few hours, or rehydrated using a few drops of water, and the same scanning procedure was performed again.

### 2.6. Examination of the stability of cellulose II hydrate in hot water

Cellulose II hydrate was treated in water at 40, 60, 80, 100, and 120 °C for a period of 1 h. After the heat treatment, the samples were cooled to room temperature while soaking in the water, and then, X-ray diffractometry measurements were performed under a RH = 100% for each sample. The measurement conditions used in the X-ray diffractometer were the same as that described in the preceding section.

## 3. Results and discussion

### 3.1. Synchrotron X-ray fiber diffraction

The synchrotron X-ray diffraction pattern of mercerized cellulose II prepared by repetitive mercerization of ramie fibers is shown in Fig. 1a. The pattern shows a high degree of crystallinity and orientation of the sample. The reflections were indexed according to a two-chain monoclinic unit cell, and the unit-cell parameters were refined as  $a = 8.10 \text{ \AA}$ ,  $b = 9.08 \text{ \AA}$ ,  $c = 10.36 \text{ \AA}$ , and  $\gamma = 117.3^\circ$ . The mercerized cellulose II was converted to cellulose II hydrate after being swollen in anhydrous hydrazine and washed with water. The X-ray diffraction pattern of cellulose II hydrate recorded under a RH = 90% is shown in Fig. 1b. The faint reflections denote a low degree of crystallinity of the sample, but the strong reflections in the lower angle region allowed us to determine a monoclinic unit cell with

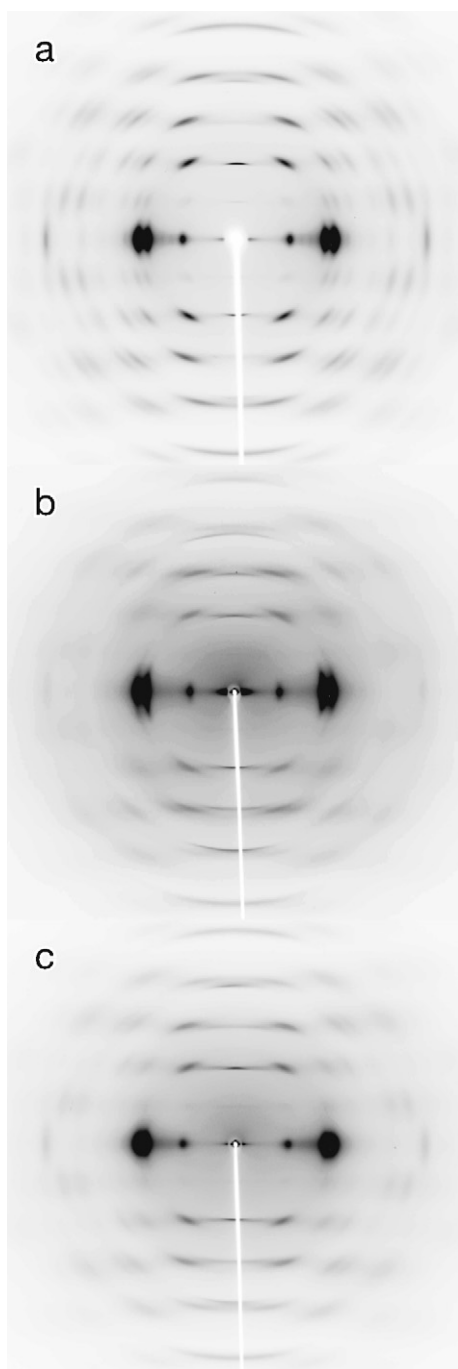


**Fig. 1.** Synchrotron X-ray fiber diffraction diagrams of: (a) mercerized cellulose II, (b) cellulose II hydrate, and (c) dried cellulose II hydrate prepared from ramie fibers. The diagram of cellulose II hydrate was recorded under a RH = 90%.

$a = 9.68 \text{ \AA}$ ,  $b = 9.95 \text{ \AA}$ ,  $c = 10.35 \text{ \AA}$ , and  $\gamma = 125.8^\circ$ . On drying the cellulose II hydrate, the X-ray diffraction pattern of the sample changed to that of cellulose II (Fig. 1c). However, the degree of crystallinity had decreased considerably compared with the initial mercerized cellulose II sample (Fig. 1a).

Some features of the X-ray diffraction pattern of cellulose II hydrate were different from the other hydrate form, Na-cellulose IV (Kobayashi et al., 2011). A major difference was the position of the innermost equatorial reflection,  $1\bar{1}0$ , where the reflections of cellulose II hydrate appeared at lower diffraction angle than that of Na-cellulose IV. When the unit-cell volumes were compared, the volume of cellulose II hydrate and Na-cellulose IV were about 19%

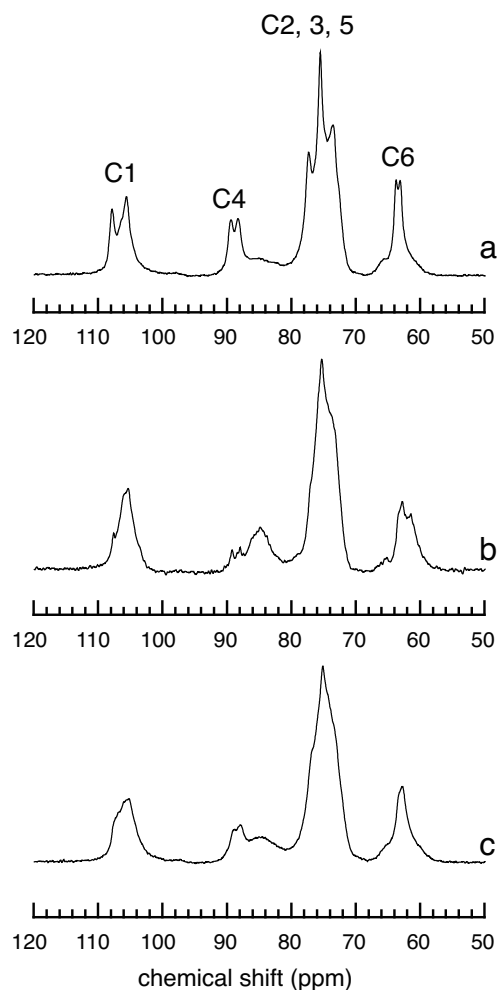


**Fig. 2.** Solid-state CP/MAS  $^{13}\text{C}$  NMR spectra of: (a) mercerized cellulose II, (b) cellulose II hydrate, and (c) dried cellulose II hydrate.

and 14% larger than that of cellulose II, respectively. This expansion of the crystalline lattice was derived from hydration, and indicated that cellulose II hydrate contained more water molecules in its crystalline lattice. On the other hand, the degree of crystallinity of cellulose II hydrate was much lower than that of Na-cellulose IV. The incorporation of more water molecules resulted in a more disordered structure.

### 3.2. Solid-state CP/MAS $^{13}\text{C}$ NMR spectroscopy

The solid-state  $^{13}\text{C}$  NMR spectra of mercerized cellulose II, cellulose II hydrate, and dried cellulose II hydrate are shown in Fig. 2. Although the conversion from cellulose II to cellulose II hydrate apparently changed the features of its spectrum, the chemical shift appeared to be identical, as evidenced by some sharp peaks, such as the C4 doublets (Fig. 2a and b). The difference occurs in the peaks derived from the organized molecules located on the crystalline surfaces, typically occurring at 82–86 ppm and 62 ppm, which became more intense and sharper in the spectrum of cellulose II hydrate. These features have also been observed in the case of Na-cellulose IV (Porro et al., 2007; Kobayashi et al., 2011), but the peak areas of cellulose II hydrate are larger than those of Na-cellulose IV. These results mean that cellulose II hydrate, as well as Na-cellulose IV, has the same molecular conformation as anhydrous cellulose II, but the crystallite size is in the order of cellulose II > Na-cellulose IV > cellulose II hydrate. The dried cellulose

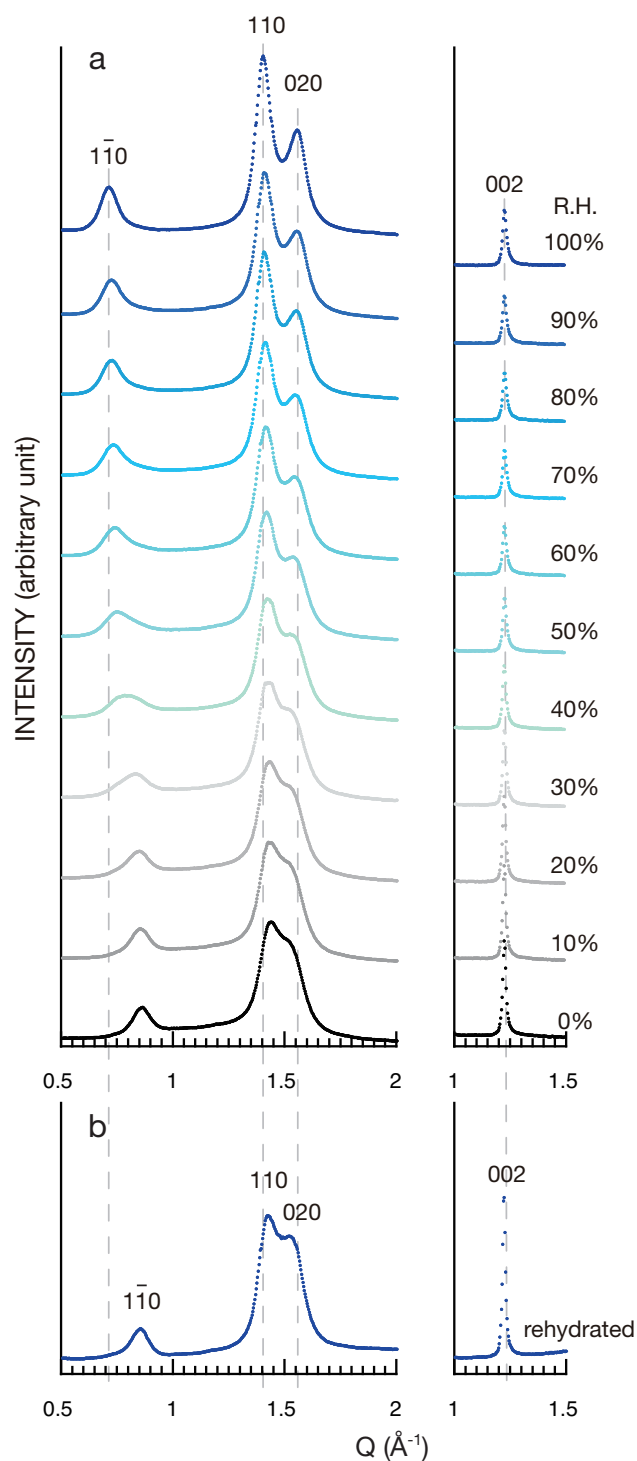


**Fig. 3.** Changes in the equatorial and meridional synchrotron X-ray fiber diffraction profiles: (a) during the drying of cellulose II hydrate, and (b) after subsequent wetting. The term  $Q$  denotes the scattering vector ( $2\pi/d$ ).

II hydrate showed a similar spectrum to mercerized cellulose II, except for the broadness of each carbon signal and the increase in peak areas of the crystalline surfaces (Fig. 2a and c). Together with the X-ray diffraction results, cellulose II hydrate showed a more disordered structure with more water molecules incorporated in the expanded crystalline lattice than did Na-cellulose IV. Thus, the cellulose II sample obtained from the dehydration of cellulose II hydrate had a more disordered structure with a lower degree of crystallinity than the initial mercerized cellulose II sample.

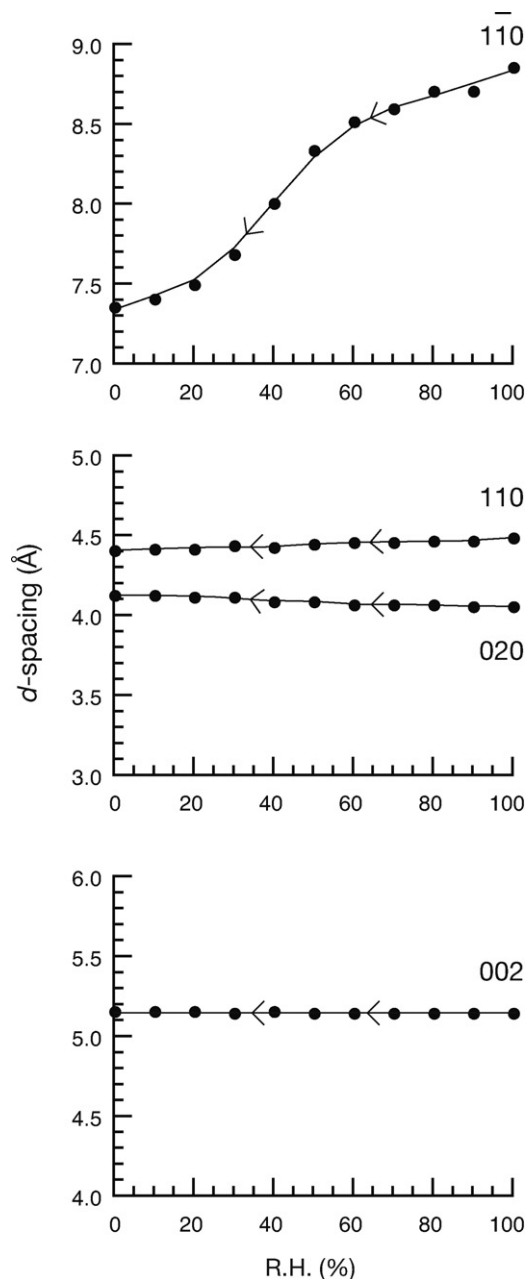


**Fig. 4.** Changes in the  $(1\bar{1}0)$ ,  $(110)$ ,  $(020)$ , and  $(002)$  plane  $d$ -spacing during the drying of cellulose II hydrate, calculated from the profiles shown in Fig. 3a.

The C6 positions of mercerized cellulose II, occurring at 63.2 and 63.9 ppm, indicated the *gt* conformation of the hydroxymethyl group (Horii et al., 1983). Because the chemical shift of cellulose II and cellulose II hydrate is almost the same, the C6 signals of cellulose II hydrate also indicated the *gt* conformation. On the other hand, the chemical shift of the peak from the crystalline surface, which occurred at about 62 ppm in the spectrum of cellulose II hydrate, corresponds to the *gg* conformation.

### 3.3. Crystal transition from cellulose II hydrate to cellulose II

The drying process of cellulose II hydrate was monitored using synchrotron X-ray diffraction. Fig. 3a shows the changes in the equatorial and meridional X-ray diffraction profiles with decreasing RH from 100% to 0%. At the beginning of the process, the equatorial and meridional profiles showed the four typical



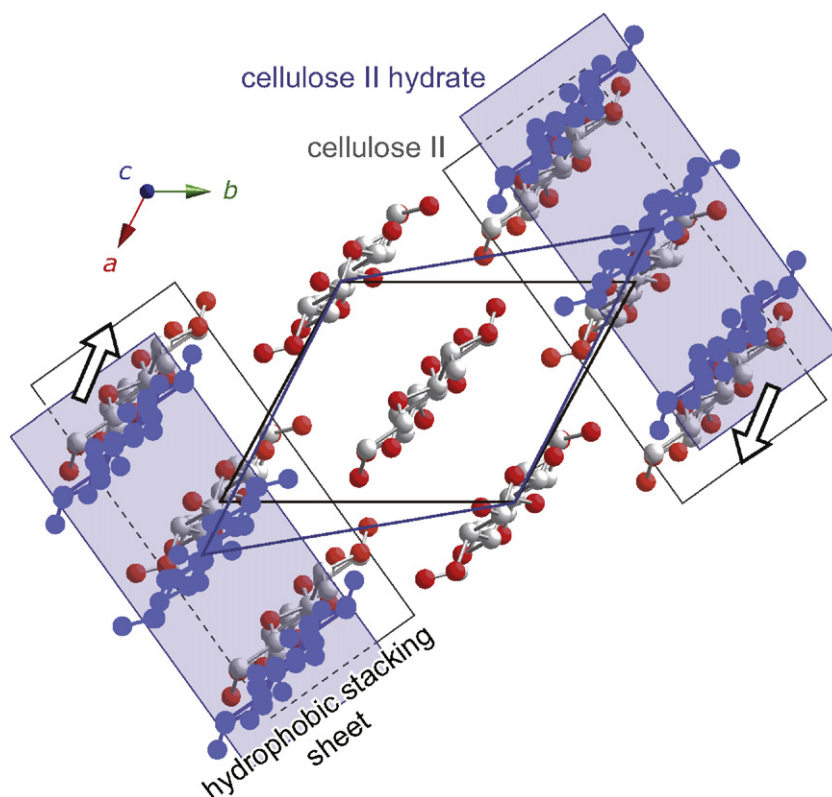


**Fig. 5.** The proposed transition mechanism from cellulose II hydrate to cellulose II based on changes in the cross-sectional unit cell during drying of cellulose II hydrate. The cellulose chains of cellulose II and cellulose II hydrate form a sheet structure that forms stacks from the hydrophobic interaction of glucopyranose rings. When cellulose II hydrate is dried, the water molecules between the sheets are released, resulting in a narrowing of the distance between the sheets. The contraction direction is orientated along the *a* axis, represented by the arrows in the figure.

reflections of cellulose II hydrate,  $1\bar{1}0$ ,  $110$ ,  $020$ , and  $002$ . The  $1\bar{1}0$  peak gradually shifted to a higher *Q* range throughout the entire drying process, while the peak width broadened until RH = 40%, and then became sharper. On the other hand, the  $110$  and  $020$  peaks shifted slightly toward higher and lower *Q* ranges, respectively, but the peak width basically remained unchanged. The  $002$  peak also showed no significant change, but it became slightly sharper. At RH = 0%, all four peaks reached the typical positions of cellulose II, indicating a completion of the transition from cellulose II hydrate to cellulose II.

The *d*-spacing of the peaks shown in Fig. 3a were calculated, and the results are shown in Fig. 4. The *d*-spacing of the  $(1\bar{1}0)$  plane was  $d_{1\bar{1}0} = 8.86 \text{ \AA}$  at RH = 100%, and this gradually decreased to  $7.36 \text{ \AA}$  at RH = 0%. The  $d_{110}$  and  $d_{020}$  values remained almost constant on drying, but decreased slightly from  $4.49$  to  $4.41 \text{ \AA}$  and increased from  $4.06$  to  $4.13 \text{ \AA}$ , respectively. The value of  $d_{002}$  was also constant at  $5.15$ – $5.16 \text{ \AA}$ . The cross-sectional unit cells at RH = 100% and 0% were determined from the  $d_{1\bar{1}0}$ ,  $d_{110}$ , and  $d_{020}$  spacings, which are shown for the unit cells of cellulose II hydrate and cellulose II in Fig. 5. Based on the change in the unit cells and the characteristic molecular sheet structure of cellulose II (Langan et al., 2001), the transition mechanism of cellulose II hydrate to cellulose II can be understood as follows. The molecular sheets stacked with hydrophobic interactions become closer to each other along the *a*-axis direction while maintaining the sheet structure (Fig. 5). In addition, a gradual change in the *d*-spacing indicates that there is no transition point. All these features of the changes occurring on the drying of cellulose II hydrate are the same for the case of Na-cellulose IV (Kobayashi et al., 2011).

Following the drying process, the samples were rehydrated using a few drops of water (Fig. 3b). The profile of the rehydrated samples was almost the same as that at RH = 0%, except for a slight

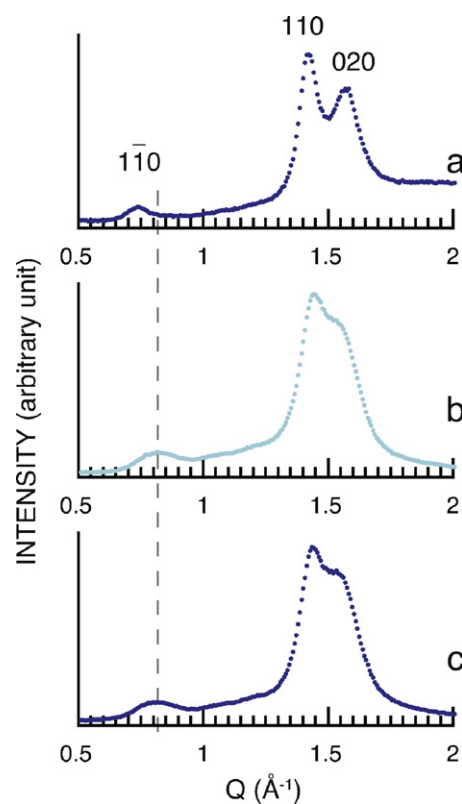


**Fig. 6.** Equatorial X-ray diffraction profiles of cellulose II hydrate: (a) at RH = 100%, (b) dried at RH = 50%, and (c) subsequently rehydrated at RH = 100%.

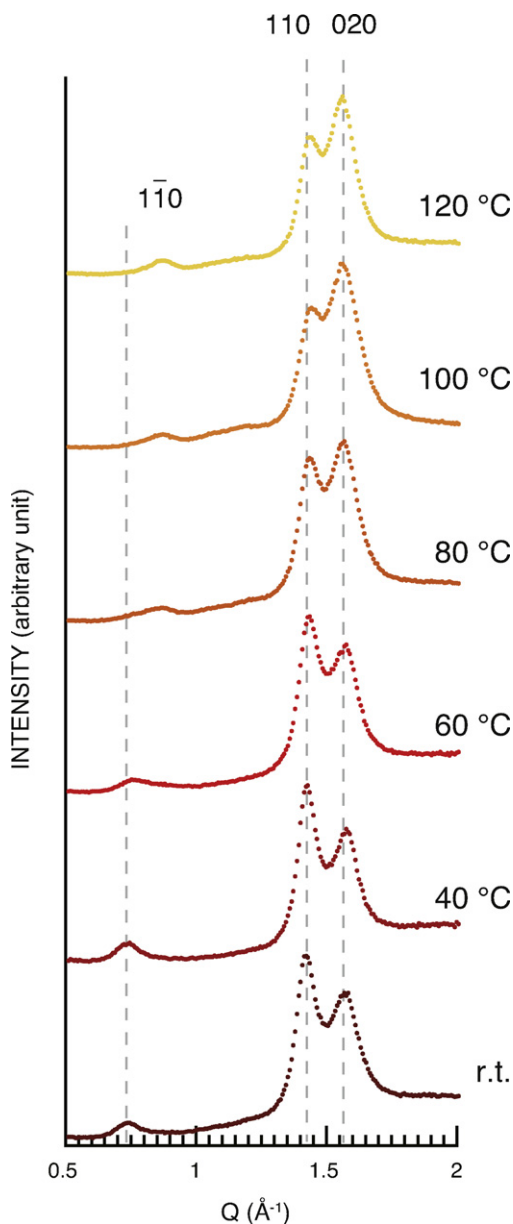


Fig. 7. Equatorial X-ray diffraction profiles of cellulose II hydrate after annealing in water for a period of 1 h at different temperatures.

sharpening of the peaks. Once dehydration was complete, the crystal structure of cellulose II was not affected by wetting, which is consistent with our previous study on Na-cellulose IV (Kobayashi et al., 2011).

Furthermore, the behavior of the sample when it was rehydrated in the middle of the transition process was also studied. Cellulose II hydrate was dried at a RH = 50%, and then it was rehydrated at RH = 100% (Fig. 6). The  $1\bar{1}0$  peak shifted to a higher Q range when the RH decreased from 100% to 50%, where some of the water molecules had been released from the crystalline lattice. When the RH increased to 100% again, or on placing a few drops of water on the sample (data not shown), the  $1\bar{1}0$  peak remained unchanged from its position at RH = 50%. This indicates that the rehydration of the half-dried sample did not convert it back to the initial hydrate form on subjecting the sample to a RH = 100% or to drops of water.

These features of the transition of cellulose II hydrate, i.e., the absence of a transition point and the irreversibility, were different from the case of other hydrate polysaccharides, e.g.,  $\beta$ -chitin

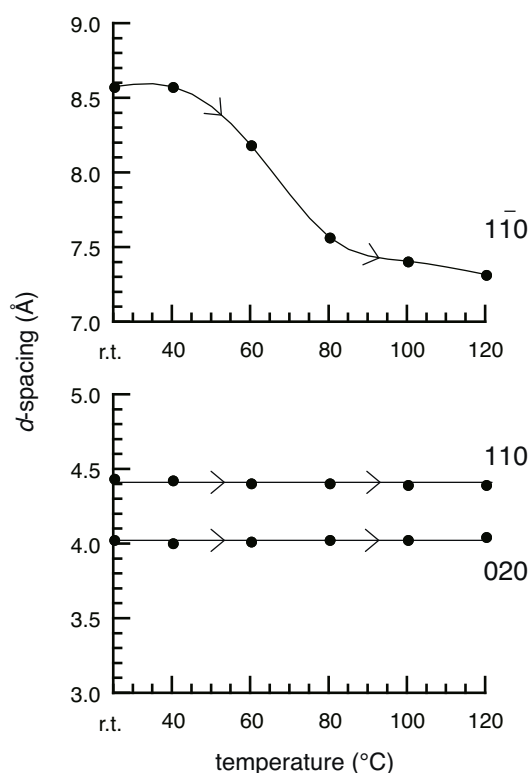


Fig. 8. Changes in the  $(1\bar{1}0)$ ,  $(110)$ , and  $(020)$  plane  $d$ -spacing on annealing cellulose II hydrate in water at various temperatures, calculated from the profiles shown in Fig. 7.

and paramylon ( $\beta$ -1,3-glucan), which show reversible transitions between their hydrate and anhydrous forms with a clear transition point (Kobayashi, Kimura, Togawa, & Wada, 2010a; Kobayashi, Kimura, Togawa, Wada, & Kuga, 2010b). As described in a previous study on Na-cellulose IV (Kobayashi et al., 2011), this different nature of the transition implies that the water molecules are incorporated disorderly into the crystalline lattice, and that they have no specific interaction with the cellulose chains. The similarity of the molecular conformation between cellulose II hydrate and cellulose II, as indicated by the  $^{13}\text{C}$  NMR spectroscopy data, is consistent with the poor relationship between the cellulose chains and the water molecules in cellulose II hydrate. A previous X-ray diffraction study also supported a random location of water molecules in the unit cell of cellulose II hydrate (Lee & Blackwell, 1981).

### 3.4. Stability of cellulose II hydrate in hot water

Samples of cellulose II hydrate kept in water were heated at various temperatures for a period of 1 h, and then the X-ray diffraction profiles of the samples were obtained at room temperature under a RH = 100% (Fig. 7). The equatorial  $1\bar{1}0$ ,  $110$ , and  $020$  peaks were located at typical positions of cellulose II hydrate in the profiles of the samples annealed at room temperature and 40 °C. However, the  $1\bar{1}0$  peak shifted slightly to a high Q range at 60 °C, and it almost reached the typical position of cellulose II at temperatures above 80 °C. The position of the  $110$  and  $020$  peaks was almost the same at all temperatures, but their intensity ratio,  $I_{110}/I_{020}$ , gradually decreased with increasing temperature. The  $d$ -spacing of these three peaks, shown in Fig. 7, was calculated, and the data are shown in Fig. 8. Similar to the drying process of cellulose II hydrate, the  $d_{1\bar{1}0}$  gradually decreased with increasing annealing temperature, while the  $d_{110}$  and  $d_{020}$  remained constant. These

results indicate that the cellulose II hydrate was converted to anhydrous cellulose II on treatment with hot water, as well as drying in air, as the hydrate form was unstable at high temperatures, even when kept in water. Since the transition gradually proceeded on annealing, the transition temperature would depend on the time of treatment.

The phenomenon of expelling hydrated water from a crystalline lattice in hot water has been observed also in other polysaccharides. Ogawa, Hirano, Miyanishi, Yui, and Watanabe (1984) prepared anhydrous chitosan by annealing a hydrate sample in water at 200 °C. Saito, Kumagai, Wada, and Kuga (2002) observed a thermal reversibility between the hydrate and anhydrous forms of  $\beta$ -chitin in water using differential scanning calorimetry and X-ray diffraction, and reported that the transition from the hydrate to the anhydrous forms occurred above 105 °C. In the recrystallization of mannan, glucomannan, and dextran from aqueous solutions, anhydrous crystals were obtained at high temperature of crystallization, while hydrated crystals were produced at low temperature (Chanzy, Excoffier, & Guizard, 1981; Chanzy, Grosrenaud, Joseleau, Dube, & Marchessault, 1982; Chanzy, Grosrenaud, Vuong, & Mackie, 1984; Chanzy, Guizard, & Sarko, 1980). The polysaccharides showed a different transition temperature, depending on their structure and stability, but dehydration caused by annealing in hot water may be a common phenomenon for hydrated polysaccharides.

#### 4. Conclusions

Samples of cellulose II hydrate were prepared from purified ramie fibers from mercerized cellulose II and a cellulose II–hydrazine complex. Synchrotron X-ray fiber diffraction under a controlled relative humidity, solid-state  $^{13}\text{C}$  NMR measurements, and X-ray diffraction analysis of annealed samples led to the following conclusions.

1. The unit cell of cellulose II hydrate expanded by up to 19% to include hydrated water compared with the anhydrous mercerized cellulose II. However, the molecular conformation of the cellulose chains was almost the same.
2. The crystal transition from cellulose II hydrate to cellulose II on dehydration occurred by drying the samples in air or annealing them in water. The hydrate structure was unstable at high temperatures, even in water.
3. In the transition process, cellulose II hydrate released hydrated water located between the hydrophobic stacking sheets, so that the sheets became close to each other along the  $a$ -axis direction while maintaining the sheet structure.
4. The crystal transition proceeded gradually without an obvious transition point, and it was irreversible. This result indicates that the hydrated water molecules have no specific interaction between the adjacent cellulose chains and are randomly located between the hydrophobic stacking sheets.

#### Acknowledgments

The synchrotron radiation experiments were performed at BL38B1 and BL40B2 in SPring-8 with the approval of the Japan Synchrotron Research Institute (JASRI). This work was supported in part by a grant from the Ministry of Agriculture, Forestry and Fisheries of Japan (Rural Biomass Research Project, BEC-BA252). K.K. acknowledges financial support from JSPS Research Fellowship for Young Scientists.

#### References

- Atalla, R. H., & VanderHart, D. L. (1984). Native cellulose: A composite of two distinct crystalline forms. *Science*, 223, 283–285.
- Chanzy, H., Excoffier, G., & Guizard, C. (1981). Single crystals of dextran. 2. High temperature polymorph. *Carbohydrate Polymers*, 1, 67–77.
- Chanzy, H., Grosrenaud, A., Joseleau, J. P., Dube, M., & Marchessault, R. H. (1982). Crystallization behavior of glucomannan. *Biopolymers*, 21, 301–319.
- Chanzy, H., Grosrenaud, A., Vuong, A., & Mackie, W. (1984). The crystalline polymorphism of mannan in plant cell walls and after recrystallisation. *Planta*, 161, 320–329.
- Chanzy, H., Guizard, C., & Sarko, A. (1980). Single crystals of dextran. 1. Low temperature polymorph. *International Journal of Biological Macromolecules*, 2, 149–153.
- Hori, R., & Wada, M. (2006). The thermal expansion of cellulose II and III<sub>II</sub> crystals. *Cellulose*, 13, 281–290.
- Horii, F., Hirai, A., & Kitamaru, R. (1983). Solid-state  $^{13}\text{C}$ -NMR study of conformations of oligosaccharides and cellulose – conformation of  $\text{CH}_2\text{OH}$  group about the exocyclic C–C bond. *Polymer Bulletin*, 10, 357–361.
- Kobayashi, K., Kimura, S., Togawa, E., & Wada, M. (2010). Crystal transition between hydrate and anhydrous  $\beta$ -chitin monitored by synchrotron X-ray fiber diffraction. *Carbohydrate Polymers*, 79, 882–889.
- Kobayashi, K., Kimura, S., Togawa, E., & Wada, M. (2011). Crystal transition from Na-cellulose IV to cellulose II monitored using synchrotron X-ray diffraction. *Carbohydrate Polymers*, 83, 483–488.
- Kobayashi, K., Kimura, S., Togawa, E., Wada, M., & Kuga, S. (2010). Crystal transition of paramyon with dehydration and hydration. *Carbohydrate Polymers*, 80, 492–498.
- Langan, P., Nishiyama, Y., & Chanzy, H. (2001). X-ray structure of mercerized cellulose II at 1 Å resolution. *Biomacromolecules*, 2, 410–416.
- Lee, D. M., & Blackwell, J. (1981a). Cellulose–hydrazine complexes. *Journal of Polymer Science: Polymer Physics Edition*, 19, 459–465.
- Lee, D. M., & Blackwell, J. (1981b). Structure of cellulose II hydrate. *Biopolymers*, 20, 2165–2179.
- Nishimura, H., & Sarko, A. (1991). Mercerization of cellulose. 6. Crystal and molecular structure of Na-cellulose IV. *Macromolecules*, 24, 771–778.
- Ogawa, K., Hirano, S., Miyanishi, T., Yui, T., & Watanabe, T. (1984). A new polymorph of chitosan. *Macromolecules*, 17, 973–975.
- Okano, T., & Sarko, A. (1984). Mercerization of cellulose. I. X-ray diffraction evidence for intermediate structures. *Journal of Applied Polymer Science*, 29, 4175–4182.
- Okano, T., & Sarko, A. (1985). Mercerization of cellulose. II. Alkali-cellulose intermediates and a possible mercerization mechanism. *Journal of Applied Polymer Science*, 30, 325–332.
- Porro, F., Bédoué, O., Chanzy, H., & Heux, L. (2007). Solid-state  $^{13}\text{C}$  NMR study of Na-cellulose complexes. *Biomacromolecules*, 8, 2586–2593.
- Saito, Y., Kumagai, H., Wada, M., & Kuga, S. (2002). Thermally reversible hydration of  $\beta$ -chitin. *Biomacromolecules*, 3, 407–410.
- Sakurada, I., & Hutino, K. (1936). Über die intramizellare quellung der zellulose durch wasser. *Kolloid-Zeitschrift*, 77, 346–351.
- VanderHart, D. L., & Atalla, R. H. (1984). Studies of microstructure in native celluloses using solid-state  $^{13}\text{C}$  NMR. *Macromolecules*, 17, 1465–1472.
- Wada, M., Okano, T., & Sugiyama, J. (1997). Synchrotron-radiated X-ray and neutron diffraction study of native cellulose. *Cellulose*, 4, 221–232.